High-resolution time series of vessel density in Kenyan mangrove trees reveal a link with climate

Anouk Verheyden[1]*, Fjo De Ridder[2], Nele Schmitz[1], Hans Beeckman[3] and Nico Koedam[1]

[1]Laboratory of General Botany and Nature Management (APNA) and [2]Laboratory of General Electricity and Instrumentation (ELEC), Vrije Universiteit Brussel, Pleinlaan, 2, B-1050 Brussels, Belgium; [3]Laboratory for Wood Biology and Xylarium, Royal Museum for Central Africa (RMCA), Leuvense Steenweg 13, B-3080 Tervuren, Belgium; *Present address: Laboratory for Wood Biology and Xylarium, Royal Museum for Central Africa (RMCA), Leuvense Steenweg 13, B-3080 Tervuren, Belgium

Summary

Author for correspondence:
A. Verheyden
Tel: +32 2769 56 12
Fax: +32 2767 02 42
Email: anouk.verheyden@africamuseum.be

• Tropical trees are often excluded from dendrochronological investigations because of a lack of distinct growth ring boundaries, causing a gap in paleoclimate reconstructions from tropical regions.
• The potential use of time series of vessel features (density, diameter, surface area and hydraulic conductivity) combined with spectral analysis as a proxy for environmental conditions in the mangrove *Rhizophora mucronata* was investigated.
• Intra-annual differences in the vessel features revealed a trade-off between hydraulic efficiency (large vessels) during the rainy season and hydraulic safety (small, more numerous vessels) during the dry season. In addition to the earlywood–latewood variations, a semiannual signal was discovered in the vessel density and diameters after Fourier transformation.
• The similarity in the Fourier spectra of the vessel features and the climate data, in particular mean relative humidity and precipitation, provides strong evidence for a climatic driving force for the intra-annual variability of the vessel features. The high-resolution approach used in this study, in combination with spectral analysis, may have great potential for the study of climate variability in tropical regions.

Key words: dendrochronology, dendroecology, East Africa, mangrove, *Rhizophora mucronata*, spectral analysis, tree rings, wood anatomy.

© *New Phytologist* (2005)

Introduction

Increasing concern about global climate change calls for the integration of regional climate data with global climate data (Watson *et al.*, 2001). However, insufficient data exist on the paleoclimate of tropical regions (Verschuren *et al.*, 2000). Recent studies conducted in Africa have used ice core records (Thompson *et al.*, 2002) and lake sediments (Johnson *et al.*, 2002) as proxies for climate variability. However, these proxies only provide limited spatial resolution over this vast continent. The environmental information archived in trees and extracted by means of dendrochronological investigations would therefore be an asset to tropical climate reconstruction.

Unlike trees of temperate regions, tropical trees have largely been excluded from dendrochronology. Despite early reports on the identification of annual growth rings in tropical trees (Coster, 1927, 1928; Berlage, 1931), dendrochronologists felt that the lack of seasonality in tropical regions hampered the application of their science (Jacoby, 1989). Because of the absence of a clear dormancy of the cambial activity, many tropical trees fail to produce distinct growth rings (Détienne, 1989; Sass *et al.*, 1995), which prevents dendrochronologists from using the classical dendrochronological method of ring width measurements (Worbes, 1990). Furthermore, when distinct growth rings are present, the periodicity of the growth rings is not necessarily annual (Détienne, 1989). Finally, when annual growth rings are identified, ring width series do not always cross-correlate (i.e. the ring width series of different trees show different patterns) or do not show a clear relationship with environmental variables (Mushove *et al.*, 1995;

February & Stock, 1998). Nonetheless, environmental information can also be archived in the wood in a variety of other ways, such as in the stable carbon and oxygen isotope ratio composition (e.g. Farquhar *et al.*, 1982; Verheyden *et al.*, 2004a), in the wood density (e.g. Hughes *et al.*, 1984; Schweingruber *et al.*, 1991) or in the wood anatomy (e.g. Baas & Carlquist, 1985; Baas, 1987).

Only a limited number of studies have used wood anatomical features in tree rings in the context of a dendrochronological investigation. However, these studies have confirmed the great potential of time series of wood anatomical features, in particular vessel density and diameter, as a proxy for environmental conditions, such as precipitation (Sass & Eckstein, 1995; Gillespie *et al.*, 1998; Pumijumnong & Park, 1999; García-Gonzales & Eckstein, 2003), temperature (Pumijumnong & Park, 1999; Fonti & García-Gonzales, 2004) and periods of flooding (Astrade & Bégin, 1997; St George & Nielsen, 2000). Eckstein (2004) has further highlighted the potential of vessel density/diameter time series for the study of intra-annual variation in climatic conditions, as well as their potential for tropical dendrochronology.

Recently, annual growth rings were discovered in *Rhizophora mucronata*, a tropical mangrove species (Verheyden *et al.*, 2004b; see the Materials and Methods section). Despite the indistinct nature of the growth ring boundaries, errors on ring width measurements were relatively small (Verheyden, 2004). However, ring width data could not be successfully cross-correlated (Verheyden, 2004). In this paper, we discuss the use of high-resolution time series of vessel features combined with spectral analysis as a proxy for environmental and climatic conditions in *R. mucronata*. In mangrove species, the vessel density and diameter were suggested to be related to the inundation frequency (Janssonius, 1950); however, this suggestion was later contradicted by van Vliet (1976) and Yáñez-Espinosa *et al.* (2001). In this study, we investigated whether the variation in vessel-related wood features (density, diameter, vessel surface area and hydraulic conductivity) is driven by a climatic factor, in particular precipitation, which in turn controls salinity and soil water potential, and relative humidity and temperature, both of which control the evaporative pulling force at the leaves. To test this hypothesis, the intra-annual variation of the vessel features was compared with the intra-annual variation in the climate variables. The potential use of our approach for tropical dendrochronology is further discussed.

Materials and Methods

Study site and sample collection

Stem discs of five *R. mucronata* Lam. trees were collected in November 1999 from Gazi Bay, Kenya (39.5° E, 4.4° S), located 40 km south of Mombasa. All samples originated from one area (~30 m²) in a basin-type forest with inundation class 2
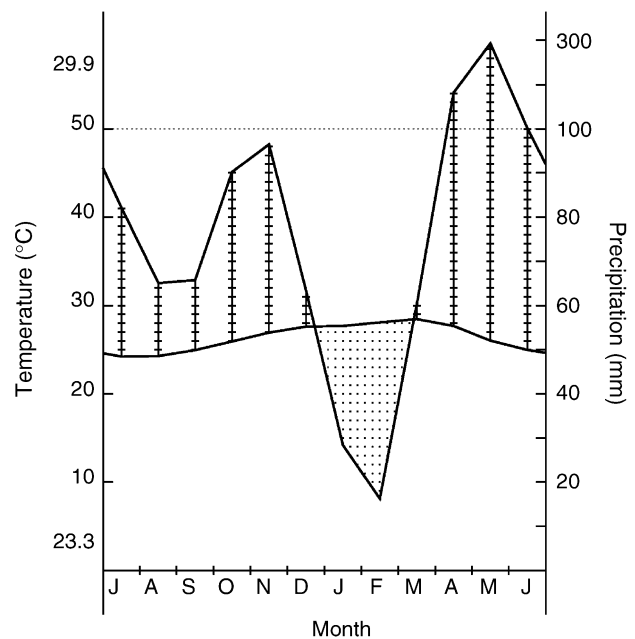

Fig. 1 Climate diagram for Mombasa, Kenya (39°36′E, 4°0′S). Adapted from Lieth *et al.* (1999).

(which corresponds to an area being inundated 50 times a month; see Tomlinson, 1986). Samples are now part of the xylarium of the Royal Museum for Central Africa (RMCA), Tervuren, Belgium (Tervuren wood collection, accession numbers Tw55890 to Tw55894). Stem diameters of the collected samples ranged between 6.6 and 10.0 cm. Trees ranged in height between 4.5 and 6.5 m and were the highest trees in this area. Only trees with a straight trunk were sampled.

Climate description

The rainfall along the Kenyan coast exhibits a bimodal distribution, which is locally expressed in terms of the long rains (from April to July) and the short rains (from October to November), with a mean annual precipitation of 1144 mm (1890–1985) (Lieth *et al.*, 1999; Fig. 1). The temperature ranges from 23.3 to 29.9°C (monthly average) with a mean annual temperature of 26.4°C (1931–1990) (Lieth *et al.*, 1999; Fig. 1). Monthly total precipitation, mean relative humidity and mean temperature data were obtained for the Mombasa region for the period between 1972 and 1999 from the Kenya Meteorological Department, Mombasa, Kenya.

Defining the growth rings

Recently, annual growth rings were discovered in *R. mucronata* from Kenya (Verheyden *et al.*, 2004b). Briefly, the growth ring consists of a low vessel density earlywood, produced during the rainy seasons, and a high vessel density latewood, produced during the dry season. The ring boundaries are indistinct and consist of a gradual change in vessel density (Fig. 2).
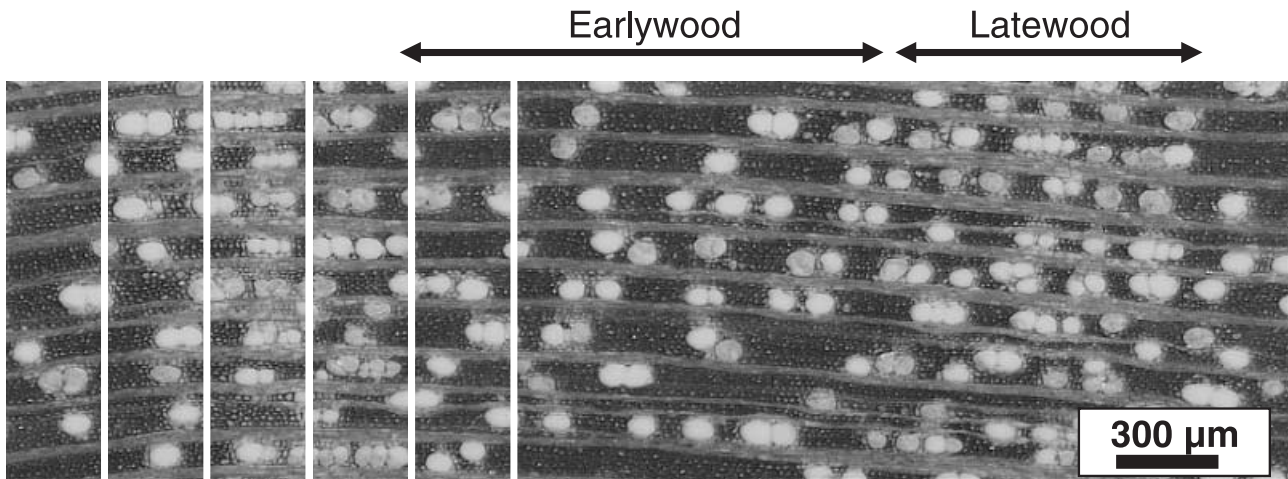
Earlywood | Latewood

300 μm

Fig. 2 Annual growth rings in the mangrove *Rhizophora mucronata* are characterized by an indistinct growth ring boundary and are composed of a low vessel density earlywood and a high vessel density latewood. High-resolution vessel density and vessel diameter profiles were obtained from measurements in adjacent windows (delineated by white vertical lines) along a radial transect from pith to bark. Each window is 300 × 2100 μm. Adapted from Verheyden *et al.* (2004b).

Sample preparation and measurements

Stem discs were air-dried and transverse sections were sanded and polished (100–1200 grit). The vessel density was measured directly on the polished wood discs, along a radial transect from bark to pith in adjacent windows (Fig. 2). Window size was set to 300 μm width and 2100 μm height. The width of the window was set arbitrarily to about 3 times the maximum height of the mean tangential diameter (~100 μm). However, increasing the resolution of the measurements by decreasing the window size did not reveal additional intra-annual information (Schmitz, 2004). Before measurements, radii were treated with white wax crayons in order to enhance the delimitation of the vessels. The vessel density was measured at an optical magnification of 12 times and the number of vessels per square millimeter was calculated. Data collection was achieved using a video camera coupled to a computer, and image analysis software (ANALYSIS 3.0; Soft Imaging System GmbH, Münster, Germany).

In addition to the vessel density, vessel tangential and radial lumen diameters were measured for sample Tw55891. Furthermore, the total vessel lumen area and the hydraulic conductivity (k_h) (assuming no embolism) were calculated from the measured vessel density and diameters. These calculated vessel variables take into account both the vessel density and the vessel diameter, and may give a better approximation of the water-transporting capacity of the wood. Lumen diameters were measured on a magnification of 12 times and a digital magnification of 200% using image analysis software (ANALYSIS 3.0). The total vessel lumen area was calculated from the vessel density multiplied by the mean vessel lumen area [$\pi \times$ (mean tangential diameter)^2]. k_h was derived from the Hagen–Poiseuille law:

$$k_h = (\pi/8\eta) \times VD \times (\text{mean TR})^4 \qquad \text{Eqn 1}$$

[m^2 MPa^{-1} s^{-1}], where η is the viscosity of water (1×10^{-9} MPa s at 20°C) VD is the vessel density (m^{-2}) and mean TR is the mean tangential radius (m) of the vessels (Sperry *et al.*, 1988).

Seasonal differences in vessel features (earlywood–latewood) were studied by classifying each of the measurements as belonging to either the earlywood or the latewood based on visual growth ring boundaries (Verheyden *et al.*, 2004b). Additional environmental signals in the intra-annual variability of the vessel features were studied by subjecting the high-resolution profiles to a spectral analysis and comparing them with the spectra obtained from climate variables.

Spectral analysis

The high-resolution profiles of the vessel features and the climate data were subjected to a Fourier transformation to detect subannual patterns. Because the vessel features were measured at equidistant intervals, a transformation needs to be applied to construct a time grid. The use of a linear transformation from this distance grid to a time grid assumes a constant annual growth rate, which is unlikely to occur in trees (see also Verheyden, 2004). In order to obtain a correct time grid, which takes into account the differences in annual growth rates, the anchor-point method was applied (Paillard *et al.*, 1996). This method makes use of annual reference points, which were obtained by superimposing the vessel density data over the indistinct growth ring boundaries and by selecting the highest peak of the vessel density in the latewood of each annual growth ring (see arrows in Fig. 3). It is important to note that the anchor-point method as applied here only corrected
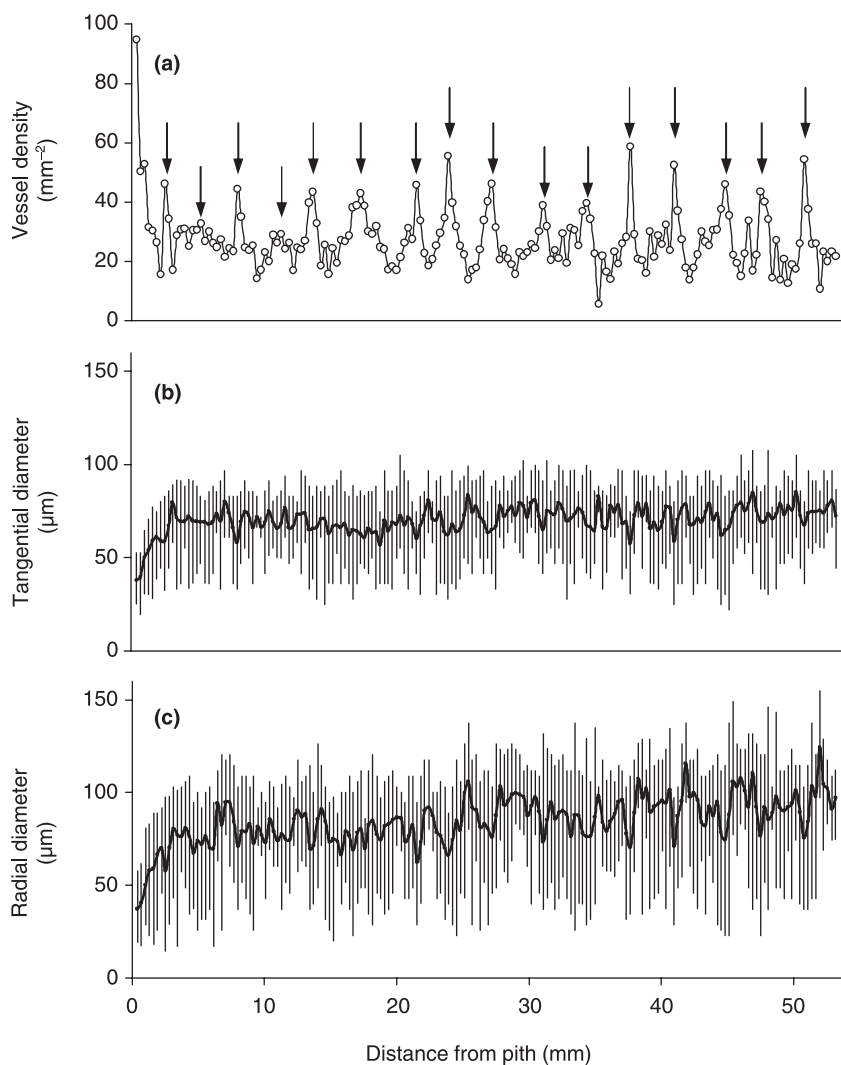
Fig. 3 *Rhizophora mucronata* vessel density (a) and mean tangential (b) and radial (c) diameters (thick solid lines) and their standard deviations (1σ, thin vertical lines) for sample Tw55891, measured along a radial transect from pith to bark. Arrows in (a) indicate the selected annual peaks in the vessel density, which are used to transform the distance grid into a time grid by applying the anchor-point method before Fourier transformation (see the Materials and Methods section).

for differences in interannual growth rates, not for differences in intra-annual growth rates (De Ridder *et al.*, 2004). The uncertainty on the periodicity was estimated by constructing a parametric model, based on a given model complexity (number of harmonics) (Pintelon & Schoukens, 2001). In this model, it is assumed that the residual, obtained from the subtraction of the model from the measurements, consists of white noise. The standard deviation of this noise was used to estimate the uncertainty level in the Fourier spectra. All processes were carried out using MATLAB 6.0 (The MathWorks Inc., Natick, MA, USA).

Statistical analysis

Differences in the vessel features between earlywood and latewood were investigated using a *t*-test for dependent samples. An evaluation of the synchronicity of the high-resolution vessel density time series obtained for the five trees was attempted by calculating Pearson correlation coefficients.

The high-resolution vessel density time series were further compared to climate variables using Pearson correlation coefficients. All analyses were carried out in STATISTICA 4.0 (StatSoft Inc., Tulsa, OK, USA).

Results

Earlywood and latewood were found to differ significantly in all the vessel variables studied. Earlywood displayed significantly lower vessel density, larger vessel diameters and lower total vessel lumen area and hydraulic conductivity than latewood (Table 1). However, the differences in vessel diameters were relatively small and exhibited a high standard deviation (Fig. 3b,c, Table 1). This indicated that both small and large vessels were present in earlywood and latewood. The difference in mean diameters was therefore a result of a higher percentage of small vessels produced during the dry season. The vessel density was significantly correlated to the radial diameter (Pearson product moment correlation coefficient $r = -0.59$,

Table 1 Seasonal differences between earlywood and latewood in vessel density, tangential and radial vessel lumen diameters, total vessel surface area and hydraulic conductivity (k_h) of the mangrove *Rhizophora mucronata*

	Mean ± SD (range)		
	Earlywood	Latewood	*t*-test
Vessel density (mm^{-2})	22 ± 5 (6–34) *n = 100*	34 ± 9 (22–59) *n = 75*	t = 11.27 P < 0.0001
Tangential vessel lumen diameter (µm)	71 ± 14 (20–108) *n = 1392*	67 ± 14 (22–108) *n = 1557*	t = 7.78 P < 0.0001
Radial vessel lumen diameter (µm)	87 ± 22 (17–155) *n = 1392*	79 ± 22 (14–146) *n = 1557*	t = 9.83 P < 0.0001
Total vessel surface area (mm^2 vessels mm^{-2} wood)	0.09 ± 0.02 (0.03–0.17) *n = 100*	0.12 ± 0.02 (0.07–0.20) *n = 75*	t = 9.02 P < 0.0001
Hydraulic conductivity (k_h) (m^2 MPa^{-1} s^{-1} × 10^{-3})	15.04 ± 4.81 (4.65–32.35) *n = 100*	17.65 ± 4.52 (8.11–28.36) *n = 75*	t = 3.65 P < 0.001

Mean, standard deviation (SD, 1σ), range and number of measurements (*n*) are given, as well as the results of the *t*-test for dependent samples.
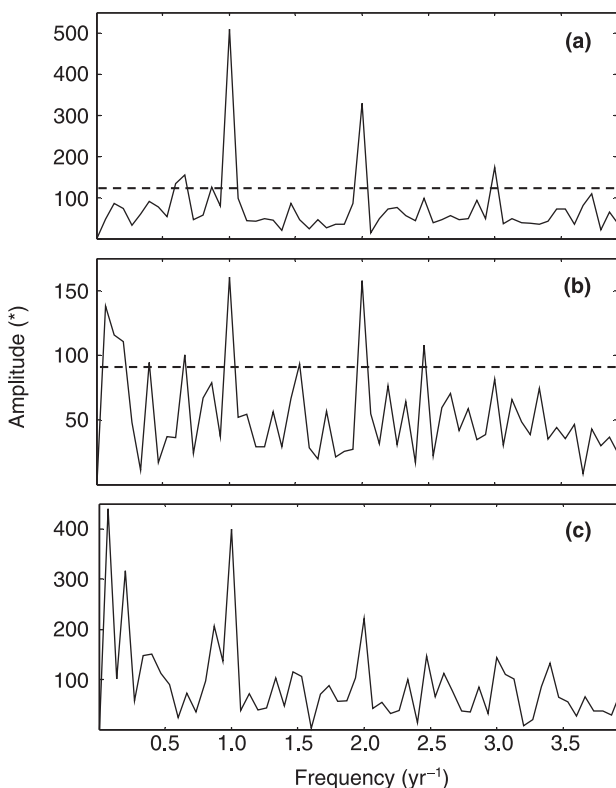

Fig. 4 Fourier spectra of the vessel density (a), the tangential vessel diameter (b) and the radial vessel diameter (c) profiles of *Rhizophora mucronata* (sample Tw55891), revealing an annual signal (frequency of 1 yr^{-1}) and a semiannual signal (frequency of 2 yr^{-1}). The anchor-point method was used to transform the distance grid into a time grid by assigning annual reference points (see Fig. 3a). Dashed lines indicate the 95% uncertainty level. However, for the radial vessel diameter spectrum, no uncertainty level could be calculated, because of trends in the raw data. (*) The units of the

n = 175, *P* < 0.001) and the tangential diameter (*r* = −0.57, *n* = 175, *P* < 0.001). Therefore, *c.* 65–70% of the variation in the vessel diameter data was independent of the variation in the vessel density, and may indicate that the combination of the two vessel variables (as total vessel lumen area and hydraulic conductivity) contains additional environmental information. The differences in vessel features between earlywood and latewood resulted in a distinct visual periodicity in the high-resolution profiles of the vessel density (Fig. 3a), but a less clear periodicity in those of the vessel diameters (Fig. 3b,c). Near the pith, juvenile wood was identified as an area with numerous small vessels; this area was excluded from further analysis.

The spectral analysis of the high-resolution profile of the vessel density (Tw55891) revealed two periodic signals, which appeared well above the uncertainty level in the Fourier spectrum (Fig. 4a): one annual and one semiannual signal (frequency of 1 and 2 yr^{-1}, respectively). The annual and semiannual signals were also observed in the spectra of the vessel diameters (Fig. 4b,c); however, the noise level was higher than in the vessel density data. In addition, signals with higher and lower frequencies (harmonics) were also present in some spectra. The vessel density profiles and their Fourier spectra of four additional samples are shown in Figs 5 and 6, respectively. All samples show the presence of an annual and a semiannual signal. Fourier transformation of the climate data also revealed two distinct periodic signals in the monthly precipitation and mean monthly relative humidity, but the semiannual signal was much reduced in the mean monthly temperature data (Fig. 7).

amplitude are the same as the units of the nontransformed data, but the absolute values are multiplied by *n* (with *n* = number of sample points) during the Fourier Transformation in MATLAB.
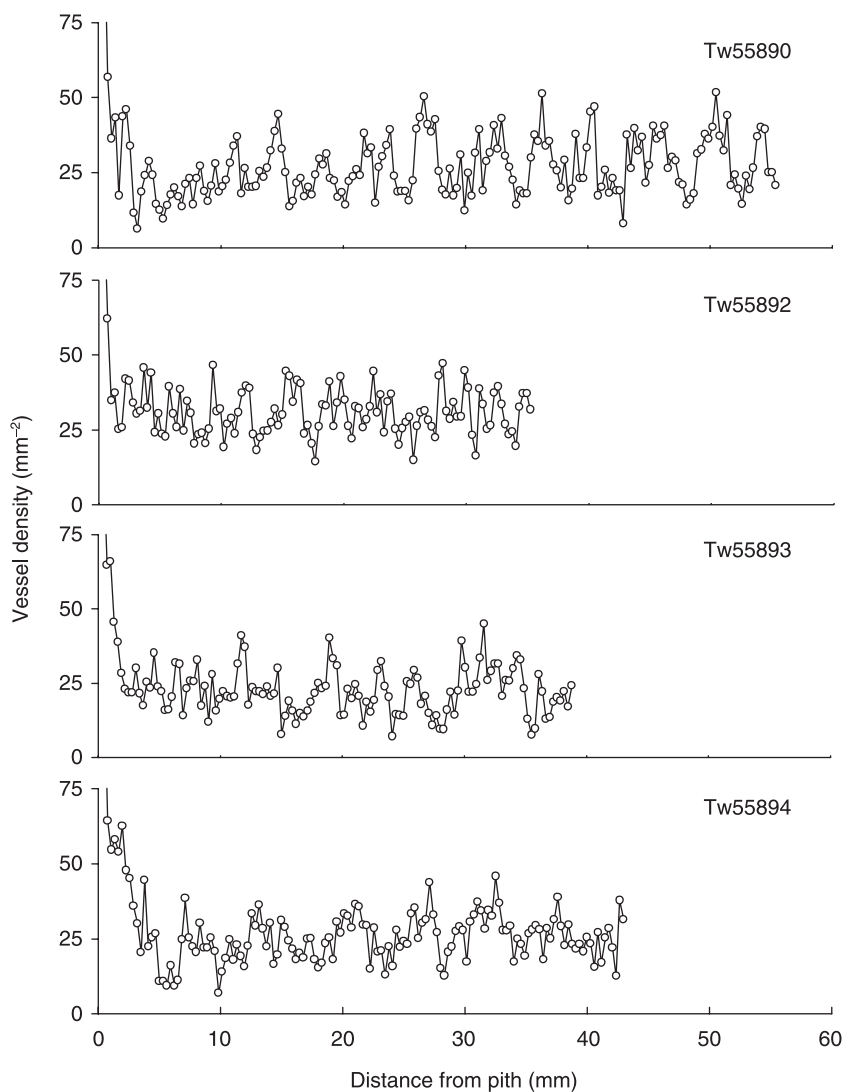
Fig. 5 Radial distribution of vessel density in the four additional *Rhizophora mucronata* stem discs collected at the same sampling site as sample Tw55891.

Table 2 Pearson correlation coefficients (*r*) calculated from comparison of the *Rhizophora mucronata* vessel density data and the mean monthly relative humidity, total monthly precipitation and mean monthly temperature

	Pearson correlation coefficient (*r*)				
	Sample				
	Tw55890	Tw55891	Tw55892	Tw55893	Tw55894
Mean monthly relative humidity	−0.60	−0.53	−0.54	−0.39	−0.54
Total monthly precipitation	ns	−0.28	−0.22	−0.28	ns
Mean monthly temperature	0.43	0.57	0.50	0.36	0.49

Coefficients are significant at $\alpha = 0.05$; ns, not significant.

Between-tree correlation coefficients (*r*) for the vessel chronologies obtained for the five trees ranged between 0.35 and 0.60. Comparison between vessel density chronologies and climate data revealed the highest correlation coefficients for the mean monthly relative humidity and mean monthly temperature (Table 2) in all five samples studied.

Discussion

Eckstein (2004) highlighted the potential of the hydrosystem of trees, in particular vessel density and diameters, as a proxy for climate reconstruction in tropical regions. In this paper, we demonstrate that high-resolution time series of vessel
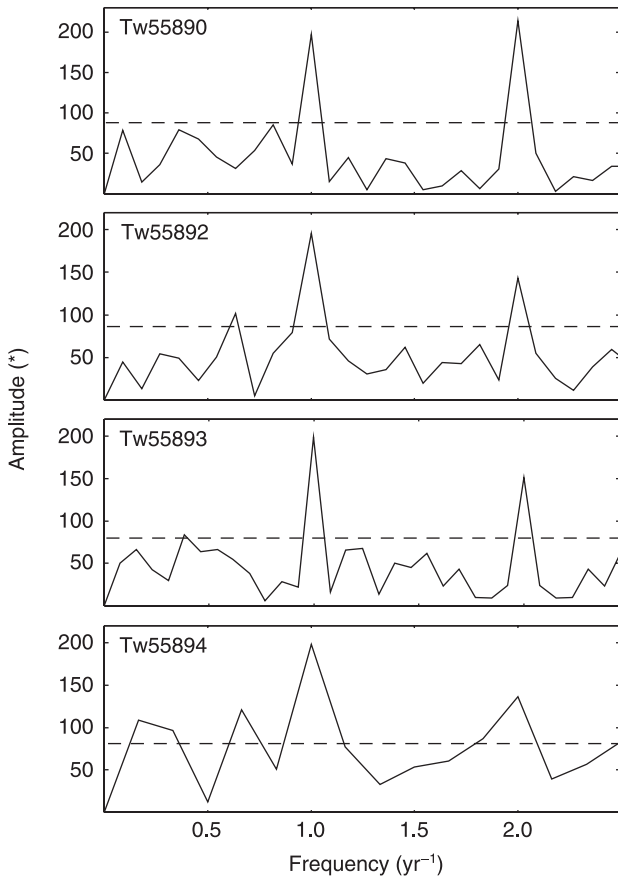
Fig. 6 Fourier spectra of the vessel density data for four additional *Rhizophora mucronata* stem discs, revealing annual (frequency of 1 yr^{-1}) and semiannual (frequency of 2 yr^{-1}) signals. Dashed lines represent the 95% uncertainty level. (*) The units of the amplitude are the same as the units of the nontransformed data, but the absolute values are multiplied by *n* (with *n* = number of sample points) during the Fourier Transformation in MATLAB.

features, combined with spectral analysis, can be used to study intra-annual variability in environmental conditions in the mangrove *R. mucronata*.

Seasonal variability in vessel features

Arnold & Mauseth (1999) found that plants can respond to changes in water availability either by changing the vessel density or the vessel diameter markedly or by changing both slightly. In *R. mucronata*, both vessel density and vessel diameter showed significant differences between earlywood and latewood, with smaller, more numerous vessels in the latewood (Table 1). However, it was the vessel density that displayed the greatest change. This is clearly reflected in the total vessel lumen area and the hydraulic conductivity, which were both higher in the latewood and therefore followed the trend of vessel density rather than vessel diameters, despite their higher theoretical dependence on the diameters (to the power of 2 for vessel lumen area and to the power of 4 for

hydraulic conductivity) (Table 1). The smaller and more numerous vessels in the latewood revealed increased hydraulic safety during the dry season. Although the mangrove soils are waterlogged, the saline conditions cause a low soil water potential, which further decreases during the dry season as a result of reduced precipitation and relative humidity as well as increased temperature and evaporation. The risk of cavitation is reduced partly by the production of smaller diameter vessels in the latewood, but mainly by an increase in the vessel density, which contributes to hydraulic safety by providing a higher percentage of vessels remaining functional when cavitation and embolism occur (Zimmerman, 1983; Tyree *et al.*, 1994).

In contrast to trees of temperate regions, the semiring porosity in *R. mucronata* is characterized by a more porous zone in the latewood. However, the increased total lumen area and hydraulic conductivity seem contrary to an ecophysiological adaptation to the dry season. Both calculated vessel variables theoretically reflect a higher water-transporting capacity of the latewood. However, Mwangi Theuri *et al.* (1999) measured lower stomatal conductivity, transpiration rates and photosynthetic rates in *R. mucronata* of Gazi Bay, Kenya (our study site) during the dry season. We therefore believe that the increased total vessel lumen area and hydraulic conductivity in the latewood do not reflect the effective water-transporting capacity in this mangrove species, but that they are artifactual consequences of the increased vessel density. The water-transporting capacity of the latewood is probably reduced by embolism occurring during the dry season. Embolism has been shown to cause a 10–15% loss in hydraulic conductivity in *Rhizophora mangle* L. at the lower range of xylem tensions occurring under field conditions (Sperry *et al.*, 1988).

Additional intra-annual variability in vessel features

The annual cyclicity in vessel density and radial and tangential diameters also appeared in the Fourier spectra of the high-resolution radial profiles. These vessel variables exhibited a distinct signal at a frequency of 1 yr^{-1} (Fig. 4). The position of this peak, at a frequency of 1 yr^{-1}, was a logical consequence of the transformation of the vessel density profile from the distance grid to a time grid (see the Materials and Methods section), and therefore does not carry environmental information. However, the fact that a clear peak was observed at this frequency (amplitude well above the uncertainty level) further illustrates the high variation in vessel variables that occurs within 1 yr, which has already been discussed following the earlywood–latewood comparison (see Table 1). In addition to the annual signal, a semiannual signal was observed at a frequency of 2 yr^{-1} (Fig. 4). The presence of this semiannual signal is remarkable in that it was only revealed by the Fourier transformation and could not be seen by investigating the wood discs or the profiles visually (see Figs 2, 3a,b,c). Fourier transformation of high-resolution vessel density profiles of the four additional stem discs from the same collection site
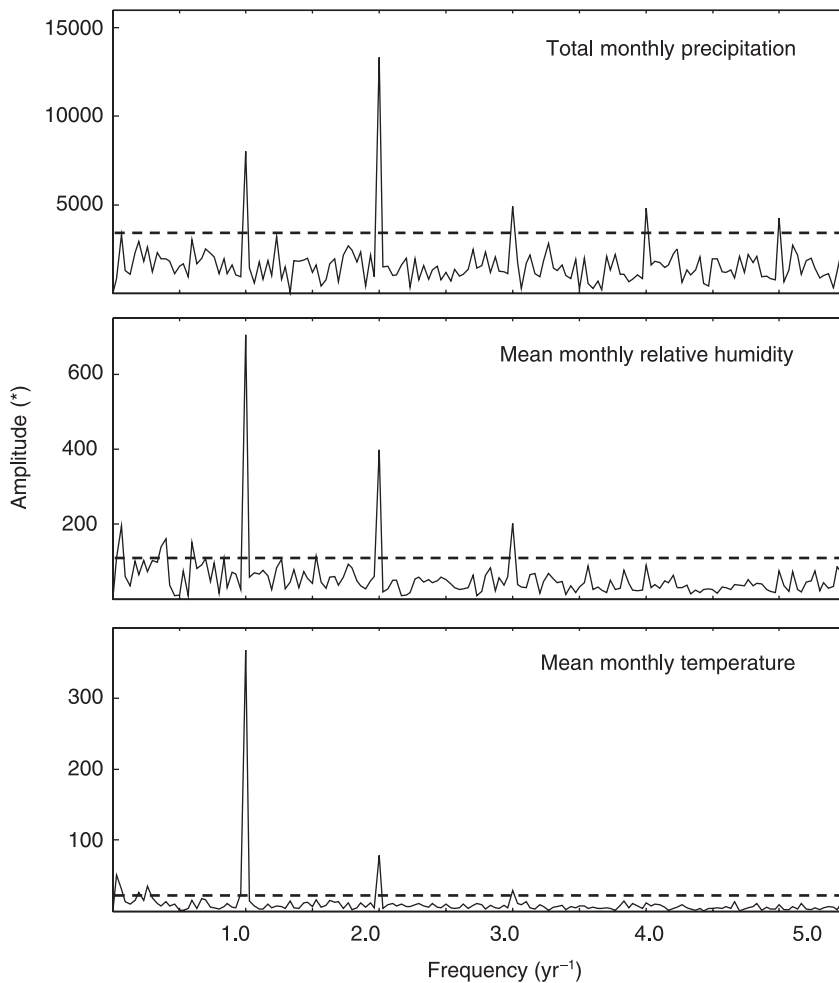
Fig. 7 Fourier spectra of the total monthly precipitation, mean monthly temperature and mean monthly relative humidity. Dashed lines represent the 95% uncertainty level. (*) The units of the amplitude are the same as the units of the nontransformed data, but the absolute values are multiplied by n (with n = number of sample points) during the Fourier Transformation in MATLAB.

further confirmed the presence of the semiannual signal (Figs 5, 6). It is interesting to note here that the periodicity in the vessel density profiles of the four additional samples was much less clear, from a visual perspective, as compared with sample Tw55891 (compare Figs 3a and 5). However, after Fourier transformation, the annual and semiannual signals clearly appeared in all samples (Fig. 6), albeit with a higher noise level as compared with the Fourier spectrum of Tw55891 (Fig. 4a).

The ecological meaning of the semiannual signal was clarified by comparing the Fourier spectra of the vessel features with the spectra of the climate variables. When the rainfall data were subjected to a Fourier transformation, the Fourier spectrum revealed an annual signal (frequency of 1 yr^{-1}) and a semiannual signal (frequency of 2 yr^{-1}) (Fig. 7). The presence of these two periodic signals in the climate data was caused by the bimodal distribution of the rainfall, which results in two rainy seasons (semiannual signal) but only one distinct dry season (annual signal) per year (Fig. 1). This semiannual signal was also present in the mean monthly relative humidity data, but was much reduced in the mean monthly temperature data, where the annual signal dominated (as demonstrated by the difference in the amplitude of the peak at frequencies of 1 and 2 yr^{-1}) (Fig. 7). The similarity in the Fourier spectra of the climate variables and the vessel features offers strong evidence that the intra-annual variations in vessel features are controlled by climatic conditions, in particular, precipitation and relative humidity, or by environmental conditions influenced by these climatic conditions (e.g. salinity). The absence of a strong semiannual signal from the temperature data makes it unlikely that the intra-annual variation in vessel features is dominated by this climate variable.

In addition to the annual and semiannual signals, a number of low- and high-frequency signals were also present in the spectra of the climate data and the vessel variables. The periodic signals (harmonics) with higher frequencies (overtones) are clearly visible in the Fourier spectrum of the precipitation data. These overtones have a much reduced amplitude in comparison to the amplitude of the annual and semiannual signals, which indicates that they are not a dominant signal in the precipitation, but rather add details to the mathematical description of the environmental data. Low-frequency signals, however, indicate long-term trends. The low-frequency signals observed in the Fourier spectra of the vessel diameters are

probably the result of an age trend, as can clearly be seen in the profile of the radial diameter (Fig. 3c). Low-frequency signals have been used to study periodic climatic events, such as the El Niño phenomenon (D'Arrigo *et al.*, 2003; Gray *et al.*, 2003) or past temperature variability (Esper *et al.*, 2002). However, the time series obtained during this study are too short (max. 17 yr) to investigate long-term climatic events accurately and are therefore not discussed further. The trees sampled for the purpose of this study were among the highest trees at the collection site. The overall young age of the trees is probably a result of the regular harvesting of the trees, as this site is easily accessible. It should be noted, however, that Verheyden *et al.* (2004b) found that *R. mucronata* trees in two forests in Kenya were relatively young overall.

Vessel density time series as a proxy for environmental conditions

The results discussed in the previous section indicate that the vessel density and diameters are very sensitive to changes in environmental conditions, because not only do they record large seasonal changes in the environment (dry season vs rainy seasons), but they also record more subtle differences, such as those occurring between the short and long rainy seasons. This offers great potential for investigating anomalies in the short rainy season separately from those in the long rainy season. Dendrochronological methods usually obtain an annual resolution (ring width measurements) or a seasonal resolution (earlywood–latewood measurements). However, the approach used in this study, in combination with spectral analysis, allows a much higher resolution. The investigation of the short rainy season would be of great value to the reconstruction of the El Niño Southern Oscillation, as El Niño events in Kenya are usually reflected as an anomaly in the short rainy season (Hastenrath & Polzin, 2003). Therefore, high-resolution time series of vessel features might be a valuable proxy in tropical dendrochronology. However, it is currently impossible to determine which of the climate data are responsible for the variation of vessel density and diameters, because of the colinearity of the precipitation, relative humidity and temperature data. Comparison of vessel density time series with climate data revealed the highest correlation coefficients for relative humidity and temperature (Table 2). The low coefficients obtained for precipitation are rather surprising. Unlike relative humidity and temperature, precipitation data have high intra- and interannual variability and are therefore more likely to be responsible for the inter- and intra-annual variability observed in the tree. While relative humidity and temperature have a direct effect on the physiological processes of the tree, the influence of precipitation on mangrove trees is probably through a lowering of the soil water salinity. However, the relationship between soil water salinity and precipitation, on the one hand, and soil water salinity and vessel density, on the other, is not necessarily (and unlikely to be) linear and may

therefore cause the low correlation coefficients observed in this study. Furthermore, additional factors will interfere with the relation between precipitation and salinity, in particular tidal cycles, topography and sediment type. The possible effect of precipitation on vessel density can only be evaluated when all these factors are considered. Although we did not manage to pinpoint which environmental variable is responsible for changes in vessel density and diameters, our results may shed light on a possible explanation for the conflicting findings of Janssonius (1950), van Vliet (1976) and Yáñez-Espinosa *et al.* (2001) (see the Introduction section). Because of the presence of inter- and intra-annual variations in vessel density and diameters, measurements from different trees and sites are only comparable when they are taken in the same year and season. However, it is very likely that previous studies used more randomized sampling in obtaining measurements, as no growth rings were recognized in those studies. This failure to recognize growth rings may have been caused by their trees having slower growth rates, which results in the disappearance of the visual distinction between high and low vessel density bands (Verheyden *et al.*, 2004b), or by a more subtle change in vessel density between earlywood and latewood.

Amongst the anatomical variables measured, the vessel density seems the most promising for extracting environmental information from *R. mucronata* wood. Vessel density measurements are easy to obtain and their Fourier spectra show a relatively low uncertainty level. In addition, no pronounced age trend was observed in the five stem discs analyzed (Figs 3–6). The vessel diameters did not show additional periodic signals and had higher uncertainty levels than the vessel density (Fig. 4). Vessel density time series overall synchronized well. Pearson correlation coefficients ranged between 0.35 and 0.60, values that are much higher than correlations obtained for ring width series for the same trees (r ranges between 0.18 and 0.36; Verheyden, 2004). However, in this study we compared high-resolution vessel density profiles, which display a clear annual cyclicity. Therefore, the degree of synchronization, especially after each profile was fit to a time scale, is expected to be higher. Future research should focus on the development of adequate statistics for comparison of high-resolution time series that display a clear periodic signal.

Potential of the high-resolution approach for tropical dendrochronology

The presence of periodic signals in the wood variables offers great potential for tropical dendrochronology, because it allows the recognition of growth rings in trees that lack distinct growth ring boundaries. Subtle seasonal changes in wood anatomical features, such as vessel density and size or fiber cell wall thickness, may not necessarily be visible to the human eye, but may still reveal periodic signals when subjected to a Fourier transformation. The key to tropical dendrochronology might therefore be to move away from the classical

New
Phytologist

dendrochronological methods of ring width measurements and to study periodic signals in high-resolution time series of wood anatomical variables.

Similar conclusions were drawn in a study on high-resolution stable carbon and oxygen isotope profiles in *R. mucronata* from Kenya (Verheyden *et al.*, 2004a). These isotope profiles also show a remarkable annual periodicity, which can be used to define growth ring boundaries in trees lacking distinct growth rings. However, unlike stable isotope analysis, wood anatomical measurements are relatively easy to obtain with a minimum of equipment required. This approach is therefore much more suitable for application by laboratories in tropical countries, which often lack the infrastructure of Western laboratories.

Acknowledgements

References

Arnold DH, Mauseth JD. 1999. Effects of environmental factors on development of wood. *American Journal of Botany* **86**: 367–371.

Astrade L, Bégin Y. 1997. Tree-ring response of *Populus tremula* L. and *Quercus robur* L. to recent spring floods of the Saône River, France. *Ecoscience* **4**: 232–239.

Baas P. 1987. Ecological trends in the wood anatomy and their biological significance. In: Schweingruber FH, ed. *Anatomy of European woods. An atlas for the identification of European trees, shrubs and dwarf shrubs.* Stuttgart, Germany: Paul Haupt, 739–762.

Baas P, Carlquist S. 1985. A comparison of the ecological wood anatomy of the floras of Southern California and Israel. *IAWA Bulletin new series* **6**: 349–353.

Berlage HP Jr. 1931. Over het verband tusschen de dikte der jaarringen van djatiboomen (*Tectona grandis* L.f.) en den regenval op Java. *Tectona* **24**: 939–953.

Coster C. 1927. Zur Anatomie und Physiologie der Zuwachszonen- und Jahresringbildung in den Tropen. *Annales du Jardin Botaniques de Buitenzorg* **37**: 49–160.

Coster C. 1928. Zur Anatomie und Physiologie der Zuwachszonen- und Jahresringbildung in den Tropen. *Annales du Jardin Botaniques de Buitenzorg* **38**: 1–114.

D'Arrigo RD, Cook ER, Mann ME, Jacoby GC. 2003. Tree-ring reconstructions of temperature and sea-level pressure variability associated with the warm-season Arctic Oscillation since AD 1650. *Geophysical Research Letters* **30**: 1549–1552.

De Ridder F, Schoukens J, Pintelon R, Gillikin DP, André L, Baeyens W, de Brauwere A, Dehairs F. 2004. Decoding non-linear growth rates in biogenic environmental archives. *Geochemistry, Geophysics, Geosystems* **5**: Q12015, doi:10.1029/2004GC000771

Détienne P. 1989. Appearance and periodicity of growth rings in some tropical woods. *IAWA Bulletin* **10**: 123–132.

Eckstein D. 2004. Change in past environments – secrets of the tree hydrosystem. *New Phytologist* **163**: 1–4.

Esper J, Cook ER, Schweingruber FH. 2002. Low-frequency signals in long tree-ring chronologies for reconstructing past temperature variability. *Science* **295**: 2250–2253.

Farquhar GD, Ball MC, von Caemmerer S, Roksandic Z. 1982. Effect of salinity and humidity on $\delta^{13}C$ value of halophytes – Evidence for diffusional isotope fractionation determined by the ratio of intercellular/atmospheric partial pressure of CO_2 under different environmental conditions. *Oecologia* **52**: 121–124.

February EC, Stock WD. 1998. An assessment of the dendrochronological potential of two *Podocarpus* species. *Holocene* **8**: 747–750.

Fonti P, García-Gonzales I. 2004. Suitability of chestnut earlywood vessel chronologies for ecological studies. *New Phytologist* **163**: 77–86.

García-Gonzales I, Eckstein D. 2003. Climatic signal of earlywood vessels of oak on a maritime site. *Tree Physiology* **23**: 497–504.

Gillespie RD, Sym SD, Rogers KH. 1998. A preliminary investigation of the potential to determine the age of individual trees of *Breonadia salicina* (Rubiaceae) by relating xylem vessel diameter and area to rainfall and temperature data. *South African Journal of Botany* **64**: 316–321.

Gray ST, Betancourt JL, Fastie CL, Jackson ST. 2003. Patterns and sources of multidecadal oscillations in drought-sensitive tree-ring records from the central and southern Rocky Mountains. *Geophysical Research Letters* **30**: 1316–1319.

Hastenrath S, Polzin D. 2003. Circulation mechanisms of climate anomalies in the equatorial Indian Ocean. *Meteorologische Zeitschrift* **12**: 81–93.

Hughes MK, Schweingruber FH, Cartwright D, Kelly PM. 1984. July–August temperature at Edinburgh between 1721 and 1975 from tree-ring density and width data. *Nature* **308**: 341–344.

Jacoby GC. 1989. Overview of tree-ring analysis in tropical regions. *IAWA Journal* **10**: 99–108.

Janssonius HH. 1950. The vessels in the wood of Javan mangrove trees. *Blumea* **6**: 465–469.

Johnson TC, Brown ET, McManus J, Barry S, Barker P, Gasse F. 2002. A high-resolution paleoclimate record spanning the past 25 000 years in southern East Africa. *Science* **296**: 113–132.

Lieth H, Berlekamp J, Fuest S, Riediger S. 1999. *Climate diagrams of the world. CD-series: climate and biosphere.* Leiden, the Netherlands: Blackhuys Publishers.

Mushove PT, Prior JAB, Gumbie C, Cutler DF. 1995. The effects of different environments on diameter growth increments of *Colophospermum mopane* and *Combretum apiculatum*. *Forest Ecology and Management* **72**: 287–292.

Mwangi Theuri M, Kinyamario JI, Van Speybroeck D. 1999. Photosynthesis and related physiological processes in two mangrove species, *Rhizophora mucronata* and *Ceriops tagal*, at Gazi Bay, Kenya. *African Journal of Ecology* **37**: 180–193.

Paillard D, Labeyrie L, Yiou P. 1996. Macintosh program performs time series analysis. *Eos, Transactions, American Geophysical Union* **77**: 379.

Pintelon R, Schoukens J. 2001. Measurement of frequency response functions using periodic excitations, corrupted by correlated input/output errors. *IEEE Transactions on Instrumentation and Measurement* **50**: 1753–1760.

Pumijumnong N, Park WK. 1999. Vessel chronologies from Teak in Northern Thailand and their climatic signal. *IAWA Journal* **20**: 285–294.

Sass U, Eckstein D. 1995. The variability of vessel size in beech (*Fagus sylvatica*) and its ecophysiological interpretation. *Trees, Structure and Function* **9**: 247–252.

Sass U, Killmann W, Eckstein D. 1995. Wood formation in two species of Dipterocarpaceae in peninsular Malaysia. *IAWA Journal* **16**: 371–384.

Schmitz N. 2004. Houtanatomie van de mangrove Rhizophora mucronata Lamk. en de relatie met de omgeving: de betekenis van de vatendichtheid voor de veiligheid van het watertransportsysteem. MSc Thesis. Brussels, Belgium: Vrije Universiteit Brussel.

Schweingruber FH, Briffa KR, Jones PD. 1991. Yearly maps of summer temperatures in Western-Europe from AD 1750 to 1975 and Western North-America from 1600 to 1982 – Results of a radiodensitometrical study on tree rings. *Vegetatio* **92**: 5–71.

Sperry JS, Tyree MT, Donnelly JR. 1988. Vulnerability of xylem to embolism in a mangrove vs inland species of Rhizophoraceae. *Physiologia Plantarum* **74**: 276–283.

St George S, Nielsen E. 2000. Signatures of high-magnitude 19th century floods in *Quercus macrocarpa* tree rings along the Red River, Manitoba, Canada. *Geology* **28**: 899–902.

Thompson LG, Mosley-Thompson E, Davis ME, Henderson KA, Brecher HH, Zagorodnov VS, Mashiotta TA, Lin PN, Mikhalenko VN, Hardy DR, Beer J. 2002. Kilimanjaro ice core records: evidence of Holocene climate change in tropical Africa. *Science* **298**: 589–593.

Tomlinson PB. 1986. *The botany of mangroves*. London, UK: Cambridge University Press.

Tyree MT, Davis SD, Cochard H. 1994. Biophysical perspectives of xylem evolution: is there a tradeoff of hydraulic efficiency for vulnerability to dysfunction? *IAWA Journal* **15**: 335–360.

Verheyden A. 2004. Rhizophora mucronata wood as a proxy for changes in environmental conditions, a study on the wood anatomy, stable isotope chemistry and inorganic composition of a Kenyan mangrove species. PhD Thesis. Brussels, Belgium: Vrije Universiteit Brussel.

Verheyden A, Helle G, Schleser GH, Dehairs F, Beeckman H, Koedam N. 2004a. Annual cyclicity in high-resolution stable carbon and oxygen isotope ratios in the wood of the mangrove tree *Rhizophora mucronata*. *Plant, Cell & Environment* **27**: 1525–1536.

Verheyden A, Kairo JG, Beeckman H, Koedam N. 2004b. Growth rings, growth ring formation and age determination in the mangrove *Rhizophora mucronata*. *Annals of Botany* **94**: 59–66.

Verschuren D, Laird KR, Cumming BF. 2000. Rainfall and drought in equatorial east Africa during the past 1100 years. *Nature* **403**: 410–413.

van Vliet GJCM. 1976. Wood anatomy of the Rhizophoraceae. *Leiden Botanical Series* **3**: 20–75.

Watson RT & the Core Writing Team (eds). 2001. *IPCC third assessment report: climate change 2001*. Geneva, Switzerland: Intergovernmental Panel for Climate Change.

Worbes M. 1990. Site and sample selection in tropical forests. In: Cook ER, Kairiukstis LA, eds. *Methods of dendrochronology. Applications in the environmental sciences*. Dordrecht, the Netherlands: Kluwer Academic Publishers, 35–40.

Yáñez-Espinosa L, Terrazas T, López-Mata L. 2001. Effects of flooding on wood and bark anatomy of four species in a mangrove forest community. *Trees, Structure and Function* **15**: 91–97.

Zimmerman MH. 1983. *Xylem structure and the ascent of sap*. Berlin, Germany: Springer-Verlag.